# High-Specific-Impulse Operation in Diverging Magnetic Field Electrostatic Thrusters with Argon Propellant

**IEPC-2019-A333**

*Presented at the 36th International Electric Propulsion Conference*
*University of Vienna • Vienna, Austria*
*September 15-20, 2019*

D. Ichihara[1], T. Matsuba[2], A. Iwakawa[3], and A. Sasoh[4]
*Department of Aerospace Engineering, Nagoya University, Nagoya, Aichi, 464-8603, Japan*

**Abstract: In this study, we developed an electrostatic thruster that had a diverging magnetic field with a cusp around a hollow cathode. Because of enhancing propellant ionization by restricting injection port, similar thrust efficiencies of 22% - 25% were obtained with different monotonic propellant; argon, krypton, and xenon. By increasing the magnetic field strength, the thrust efficiency was improved owing to the suppression of the discharge current while an almost constant thrust was maintained. A specific impulse of more than 3000 s with thrust efficiency greater than 30% was obtained.**

## Nomenclature

| | | |
|---|---|---|
| $B$ | = | magnetic field strength |
| $e$ | = | elementary charge |
| $F$ | = | thrust |
| $g$ | = | gravitational acceleration |
| $I_{sp}$ | = | specific impulse |
| $J_d$ | = | discharge current |
| $J_i$ | = | ion beam current |
| $J_k$ | = | keeper current |
| $m_i$ | = | ion mass |
| $\dot{m}_a$ | = | anode mass flow rate |
| $\dot{m}_c$ | = | cathode mass flow rate |
| $\dot{m}_t$ | = | total mass flow rate (= $\dot{m}_a + \dot{m}_c$) |
| $V_d$ | = | discharge voltage |
| $V_k$ | = | keeper voltage |
| $z$, $r$ | = | cylindrical coordinates |
| $\eta$ | = | thrust efficiency |

## I. Introduction

For deep-space exploration missions[1]or near-Earth orbit transfers[2], a propulsion system with high exhaust velocity (namely, high specific impulse) is necessary especially in high delta-v missions to enhance the payload ratio. Electric space propulsion can accelerate ions to an exhaust speed level that is not achieved by chemical propulsion[3].Among the electric space propulsions, electrostatic thrusters accelerate ions without collisions, thereby yielding a high thrust efficiency over 50%. In principle, the specific impulse in the electrostatic acceleration is in proportion to the square root of $V_d/m_i$. The typical specific impulse for ion engine[4], Hall thrusters[5], cylindrical Hall

[1] Research associate, Department of Aerospace Engineering, daisuke.ichihara@mae.nagoya-u.ac.jp.
[2] Graduate Student, Department of Aerospace Engineering, matsuba@fuji.nuae.nagoya-u.ac.jp.
[3] Lecturer, Department of Aerospace Engineering, iwakawa@nuae.nagoya-u.ac.jp.
[4] Professor, Department of Aerospace Engineering, akihiro.sasoh@mae.nagoya-u.ac.jp.

thrusters[6], and High Efficiency Multistage Plasma thrusters[7] are 4000 s, 1500 – 3500 s, 2000 s, and 3000 s, respectively. Although these electrostatic thrusters provide high specific impulse with high thrust efficiency, these performances can be achieved only when xenon is used as a propellant primary because of the favorable tradeoff between availability, atomic mass, ionization energy, and ionization cross-section[8]. However, the excessive usage of xenon is almost prohibitively expensive as compared to other viable alternatives. Currently, xenon costs 1440 U.S. dollars/kg, which is 240 times higher than the cost of argon[9]. One option to achieve the high-specific impulse operation with a cheaper cost is the usage of argon. Compared to xenon, argon has a one-third of weight, but higher ionization energy with smaller ionization cross-section. Hence, an argon propellant operation has demonstrated worse thrust performances that the conventional xenon propellant operation[10]. In order to enhance the argon propellant ionization, Ichihara et al. [11] developed the diverging-magnetic-field electrostatic thruster (DM-EST), which comprised a diverging magnetic field between a ring anode that was coaxially set on the center axis and a hollow cathode set at a cusp of the applied magnetic field. The thruster used the basic structure of a helicon electrostatic thruster[12]. We developed the "near-anode ionization scheme"[13], in which the propellant was injected through an annular slit on the inner surface of a ring anode, so that efficient ionization and ion acceleration from the near-anode to cathode potential were realized. In order to evaluate the thrust performances, we newly developed two DM-ESTs. For applying the diverging magnetic field, one used only permanent magnets and yokes and another one used two electro-magnet coils to vary the strength with keeping magnetic field geometry. In this talk, the characteristics of thrust performances with monoatomic propellants; argon, krypton, and xenon and ion beam properties are presented.

## II. Experimental Apparatus

### A. Thruster Heads

Figure 1 shows a schematic of the permanent magnet diverging magnetic field electrostatic thruster (PM-DM-EST). The thruster shares common features with the thruster of Ref. 13; a ring anode on the center axis and an off-axis hollow cathode set in a cusp of the applied magnetic field in the downstream. Inside the anode, a ceramic plate made of boron nitride plugs the passage of the propellant, except for the 1.5-mm-wide annular slit along the inner surface of the ring anode. The cylindrical coordinates ($z$, $r$), where $z$ and $r$ are the axial and radial coordinates, respectively, are defined as shown in Fig.1. By using the permanent magnets and yokes, the magnetic field strength were 75 mT at ($z$, $r$) = (0 mm, 0 mm) and 250 mT at ($z$, $r$) = (0 mm, 13.5 mm). The hollow cathode located at ($z$, $r$) = (32 mm, 37 mm). More detailed description about the PM-DM-EST was found in our previous report[14].

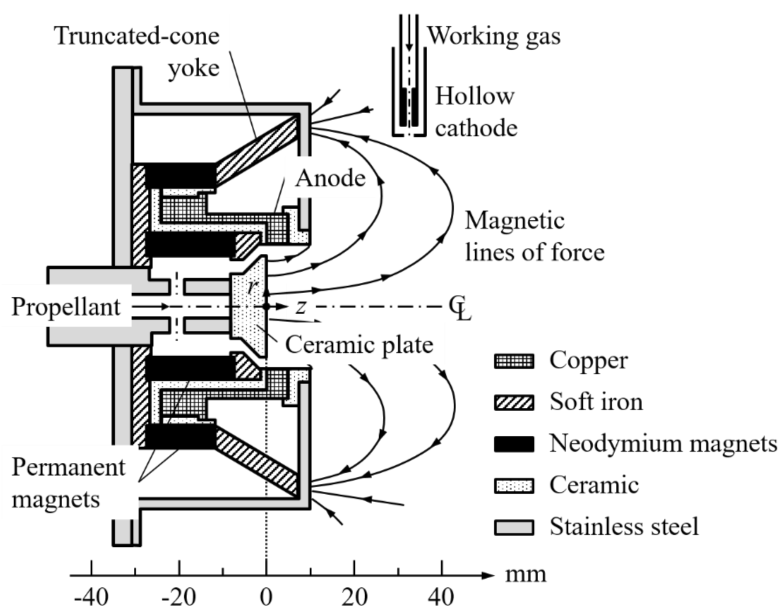


**Figure 1. Schematic of a permanent magnet DM-EST (PM-DM-EST)[14].**

Figure 2 shows a schematic of the electro-magnet diverging magnetic field electrostatic thruster (EM-DM-EST). The diverging magnetic field was applied between the ring anode and the off-axis hollow cathode. In order to vary the magnetic field strength with keeping the magnetic field geometry, two solenoid coils with supplied currents in the opposite direction to each other were used. By changing the coil currents, magnetic field strength at the center of the coil 1 was varied as 100 mT, 150 mT, and 200 mT. The ring anode had an inner diameter of 30 mm and an effective length of 10 mm. Inside the ring anode, a ceramic plate was installed to form a 1.5-mm-width annular slit for propellant injection. The hollow cathode located at ($z$, $r$) = (172 mm, 115 mm).

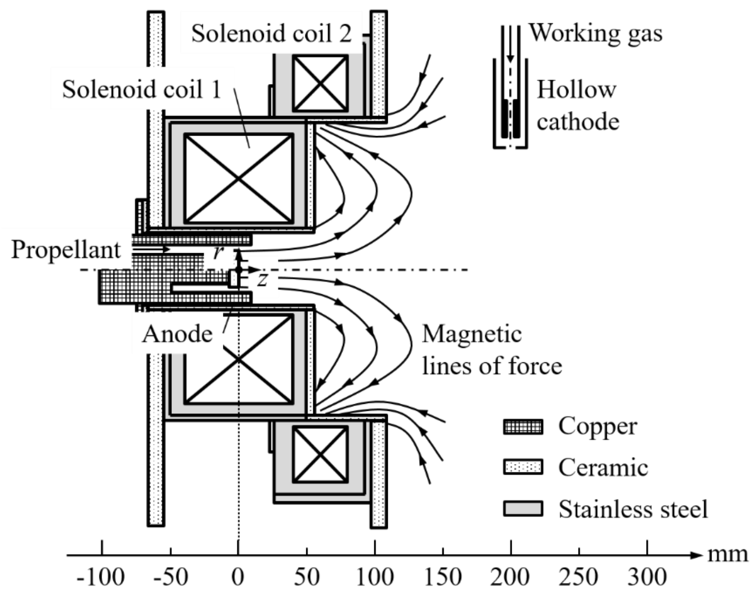


**Figure 2. Schematic of an electro-magnet DM-EST (EM-DM-EST).**

## B. Thrust Measurement and Diagnostics

For thrust performance evaluation, thrust and ion beam current were measured by a pendulum type thrust stand and a nude Faraday probe, respectively. Because the details of each measurement system were described in our previous articles[13, 14], here we note the features of each equipment briefly.

### 1. Thrust Measurement

Pendulum type thrust stands with different types of fulcrums were used to directly measure the thrust. For PM-DM-EST, the fulcrum point was supported by two knife-edges[14] and for EM-DM-EST, the fulcrum was supported by a vacuum bellows[15]. The calibrated conversion factors were 174 ± 0.33 mN/V for the knife-edge pendulum and 259 ± 3.2 mN/V for the bellows pendulum. Both thrust stand showed the same resolution of 0.2 mN, which was less than 3% of the minimum thrust value. The tare force was measured beforehand and was taken into account in the correction of thrust measurement.

### 2. Ion Beam Current Measurement

The same nude Faraday probe and its measuring circuit as in the previous work[13] were used to measure $J_{\mathrm{i}}$. The swing-arm length was 375 mm with the fulcrum at ($z$, $r$) = (95 mm, 0 mm) for PM-DM-EST and 250 mm at ($z$, $r$) = (109 mm, 0 mm) for EM-DM-EST. The swing center was set at thruster exit. The definition of $J_{\mathrm{i}}$ was also described in Ref.13.

# III. Experimental Results and Discussions

## A. Operating Conditions

Table 1 summarizes the investigated operating conditions. Gas purity was 99.9999% for argon (Ar), and it was 99.995% for krypton (Kr) and Xe. The uncertainties in $\dot{m}_{\mathrm{a}}$, $V_{\mathrm{d}}$, and $J_{\mathrm{d}}$ were ± $10^{-2}$ mg/s, ± 2.0 V, and ± 51 mA, respectively. All experiments were conducted in a stainless-steel vacuum chamber. Under the operating conditions, background pressure was maintained in low-to-middle $10^{-2}$ Pa range

**Table 1. Operating conditions.**

| Parameter | Unit | PM-DM-EST | | | EM-DM-EST |
|---|---|---|---|---|---|
| Propellant | - | Ar | Kr | Xe | Ar |
| $\dot{m}_a$ | mg/s | 1.2 | 1.7 | 1.3 | 0.62 |
| $\dot{m}_c$ | mg/s | 0.14 | 0.31 | 0.48 | 0.14 |
| $\dot{m}_t$ | mg/s | 1.34 | 2.01 | 1.78 | 0.76 |
| $V_d$ | V | 150-350 | 175-275 | 175-275 | 125-250 |
| $B$ | mT | 75 | 75 | 75 | 100-200 |
| $J_k$ | A | 2.0 | 2.0 | 2.0 | 2.0 |

## B. Operation Characteristics of PM-DM-EST

Figure 3 shows the $V_d$ dependence of $J_i/(e\dot{m}_t/m_i)$, $\eta$, and $I_{sp}$ with different propellant species in PM-DM-EST. For a singly charged ion, the value $J_i/(e\dot{m}_t/m_i)$ represents the propellant utilization efficiency. In all $V_d$, $J_i/(e\dot{m}_t/m_i)$ of Kr and Xe propellant exceeded unity. For Ar propellant, $J_i/(e\dot{m}_t/m_i)$ increased with increasing $V_d$. Due to the near-anode ionization scheme, $J_i/(e\dot{m}_t/m_i)$ reached unity when $V_d$ = 250 V even with argon propellant.

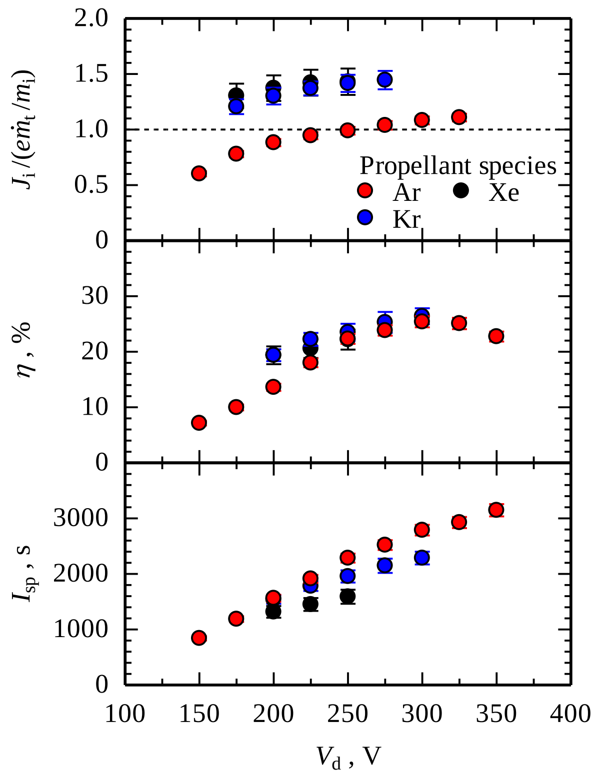


**Figure 3. The $V_d$ dependence of $J_i/(e\dot{m}_t/m_i)$, $\eta$, and $I_{sp}$ with different propellant species in PM-DM-EST. Operating conditions are summarized in Table 1.**

The thrust efficiency and specific impulse were defined as follows;

$$\eta \equiv \frac{F^2}{2\dot{m}_t\left(J_d V_d + J_k V_k\right)}, \tag{1}$$

$$I_{sp} \equiv \frac{F}{\dot{m}_t g}. \tag{2}$$

Calculated $\eta$ and $I_{sp}$ are also shown in Fig.3. Regardless of the propellant species, $\eta$ increased with increasing $V_d$. When $V_d$ = 250 V, $\eta$ was overlapped with each other at 22%. Ar propellant showed the maximum $\eta$ of 25% at $V_d$ = 300 V and gradually decreased as increasing $V_d$. Due to the near-anode ionization scheme, propellant ionization was enhanced and similar thrust efficiency was obtained with different propellant species. On the other hand, $I_{sp}$ depended propellant species and monotonically increased with increasing $V_d$. As mentioned in Introduction, $I_{sp}$ is proportional to $(V_d/m_i)^{½}$. Hence, at the same $V_d$, lighter propellant showed higher $I_{sp}$; at $V_d$ = 250 V, $I_{sp}$ was 2200 s, 1900 s, and 1500 s with Ar, Kr, and Xe operation, respectively. The maximum $I_{sp}$ was 3100 s in Ar propellant operation.

### C. Operation Characteristics of EM-DM-EST

Figure 4 shows the $V_d$ dependence of $F$, and $J_d$ with different $B$ in EM-DM-EST. $F$ increased with increasing $V_d$. Because an electrostatic acceleration has no dependency on $B$, $F$ was overlapped within the uncertainty regardless of $B$. On the other hand, $J_d$ depended $B$ that higher $B$ showed smaller $J_d$. At $V_d$ = 250 V, $J_d$ = 8.0 A, 7.0 A, and 6.0 A for $B$ = 100 mT, 150 mT, and 200 mT, respectively. By increasing $B$, electron motion crossing the magnetic lines of force was suppressed and $J_d$ was decreased. However, $J_d$ maintained still higher value than that of current equivalent of anode flow rate $e\dot{m}_a/m_i$.

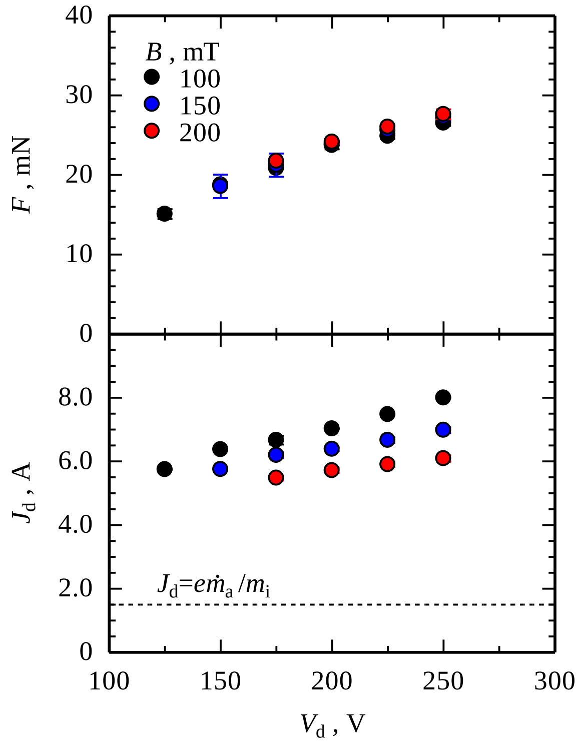


**Figure 4. The $V_d$ dependence of $F$, and $J_d$ with different $B$ in EM-DM-EST, $\dot{m}_a$ = 0.62 mg/s, $\dot{m}_c$ = 0.14 mg/s.**

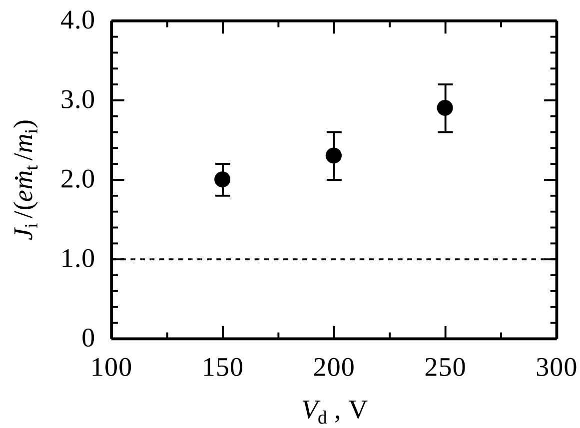


**Figure 5. The $V_d$ dependence of $J_i/(e\dot{m}_t/m_i)$ in EM-DM-EST, $\dot{m}_a$ = 0.62 mg/s, $\dot{m}_c$ = 0.14 mg/s, $B$ = 100 mT.**

The values of $J_i/(e\dot{m}_t/m_i)$ with respect to $V_d$ is shown in Fig. 5. In EM-DM-EST, $J_i/(e\dot{m}_t/m_i)$ were much greater than unity in all $V_d$. Although the effect of secondary electron emission from the collector surface was not corrected, this results strongly suggested that multiply charged ions had a non-negligible fraction in the extracted ion beam. The experiment which can estimate multiply-charged ion fractions have not been conducted.

Figure 6 shows thrust performances with different $B$ in EM-DM-EST. We used the same definitions for $\eta$ and $I_{sp}$ as shown in Eqs. (1) and (2), respectively. Because $J_d$ decreased with increasing $B$ while $F$ showed no dependency on $B$ (see Fig. 4), $\eta$ increased as increasing $B$. At $V_d$ = 250 V, $\eta$ = 22%, 27%, and 31% for $B$ = 100 mT, 150 mT, and 200 mT, respectively. It is not shown but the thrust-to-power ration ranged from 13 mN/kW to 22 mN/kW. Similar to $F$ variation, $I_{sp}$ showed no dependence on $B$ and increased monotonically with increasing $V_d$. The maximum $I_{sp}$ was 3600 s at $V_d$ = 250 V. Compared with previous argon propellant operations in Hall thrusters[10,16, 17], both the obtained $I_{sp}$ and $\eta$ were higher than those of previous reports. Although $V_d$ was up to 250 V, the maximum $I_{sp}$ was higher than that of conventional xenon-Hall thrusters even with a 1.0-kV discharge voltage operation[5].

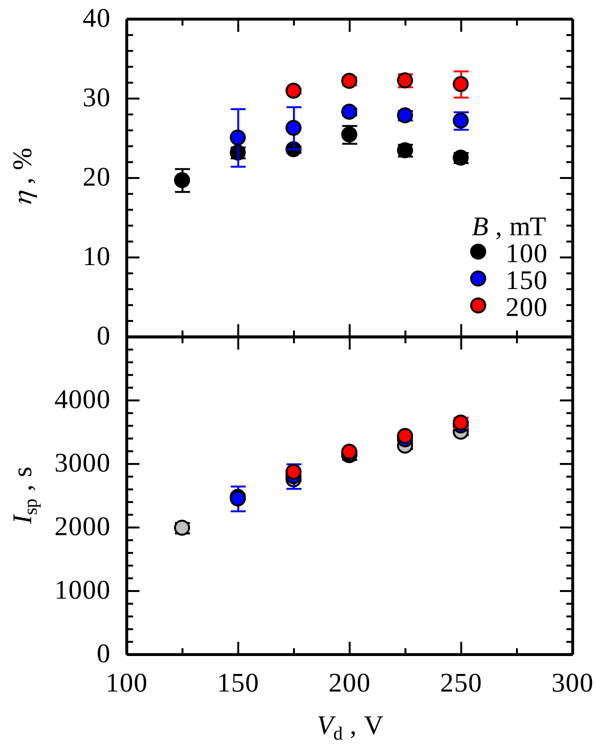


**Figure 6. The $V_d$ dependence of $\eta$, and $I_{sp}$ with different $B$ in EM-DM-EST, $\dot{m}_a$ = 0.62 mg/s, $\dot{m}_c$ = 0.14 mg/s.**

## IV. Conclusion

We demonstrated the similar thrust performances with different monotonic propellants and its improvement by applying a strong diverging magnetic field in DM-ESTs. Due to the near-anode ionization scheme, injected argon gas were fully ionized and electrostatically accelerated more than 3000 s of $I_{sp}$. Although $V_d$ was up to 250 V, the maximum $I_{sp}$ was higher than that of conventional xenon-Hall thrusters even with a 1.0-kV discharge voltage operation. Regardless of the propellant species, similar thrust efficiencies of 22% - 25% were obtained. By strengthening the magnetic field, electron motion crossing the magnetic lines of force was suppressed and hence, thrust efficiency was increased up to 31% even with argon propellant. Compared with previous argon propellant operations in Hall thrusters, both the obtained $I_{sp}$ and $\eta$ were higher than those of previous reports.

## Acknowledgments


his research was supported by the Japan Society for Promotion of Science, Grants-in-Aid for Scientific Research (A) No. 18H03813 and for Young Scientists No. 18K13925. The authors thank A. Saito, Y. Nakanishi, S. Goto, Y. Adachi, and R. Yamamoto at the Technical Division, Nagoya University, for their valuable technical assistance.

## References


[1]Oh, D. Y., Snyder, J. S., Goebel, D., M., Hofer, R. R., and Randolph, T., M., “Solar Electric Propulsion for Discovery-Class Missions,” *Journal of Spacecraft and Rockets*, Vol. 51, No. 6, 2014, pp. 1822-1835.

[2]Rathsman, P., Kugelberg, J., Bodin, P., Racca, G. D., Foing, B., Stagnaro, L., “SMART1: Development and Lessons Learnt,” *Acta Astronautica*, Vol. 57, May. 2005, pp. 455-468.

[3]Mazouffre, S., “Electric Propulsion for Satellites and Spacecraft: Established Technologies and Novel Approaches,” *Plasma Sources Science and Technology*, Vol. 25, No. 3, 2016, Paper 033002.

[4]Snyder, J. S., Goebel, D. M., Hofer, R. R., and Polk, J. E., “Performance Evaluation of the T6 Ion Engine,” *Journal of Propulsion and Power*, Vol. 28, No. 2, 2012, pp. 506-513.

[5]Hofer, R., R., Jankovsky, R. S., and Gallimore, A. D., “High-Specific Impulse Hall Thrusters, Part 1: Influence of Current Density and Magnetic Field,” *Journal of Propulsion and Power*, Vol. 22, No. 4, 2006, pp. 721-731.

[6]Kim, H., Lim, Y., Hhoe, W., and Seon, J., “Effect of Multiply Charged Ions on the Performance and Beam Characteristics in Annular and Cylindrical Type Hall Thruster Plasmas,” *Applied Physics Letters*, Vol. 105, No. 14, 2014, Paper 144104.

[7]Reijen, B. van., Lazurenko, A., Weis, S., Heidemann, R., Jaderspeck, J., Genovese, A., Holtmann, P., Ruf, K., and Püttmann, N., “Scalability of the HEMP-T Technology for Station Keeping and Orbit Rising,” *34th International Electric Propulsion Conference*, IEPC-2015-344, Kobe-Hyogo, Japan, 2015.

[8]Sorokin, A. A., Shmaenok, L. A., and Bobashev, S. V., “Measurements of Electron-Impact Ionization Cross Sections of Argon, Krypton, and Xenon by Comparison with Photoionization,” *Physical Review A*, Vol. 61, No. 2, 2000, Paper 022723.

[9]Kieckhafer, A., and King, L. B., “Energetics of Propellant Options for High-Power Hall Thrusters,” *Journal of Propulsion and Power*, Vol. 23, No. 1, 2007, pp. 21-26.

[10]Yamazaki, J., Yokota, S., and Shimamura K., “Performance Enhancement of an Argon-based Propellant in a Hall Thruster,” *Vacuum*, Vol. 167, 2019, pp. 520-523.

[11]Ichihara, D., Uchigashima, A., Iwakawa, A., and Sasoh, A., “Electrostatic Ion Acceleration across a Diverging Magnetic Field,” *Applied Physics Letters*, Vol. 109, No. 5, 2016, Paper 053901.

[12]Harada, S., Baba, T., Uchigashima, A., Yokota, S., Iwakawa, A., Sasoh, A., Yamazaki, T., and Shimizu, H., “Electrostatic Acceleration of Helicon Plasma using a Cusped Magnetic Field,” *Applied Physics Letters*, Vol. 105, 2014, Paper 194101.

[13]Ichihara, D., Iwakawa, A., and Sasoh, A., “Effects of Magnetic Field Profile near Anode on Ion Acceleration Characteristics of a Diverging Magnetic Field Electrostatic Thruster,” *Journal of Applied Physics*, Vol. 122, No. 4, 2017, Paper 043302.

[14] Ichihara, D., and Sasoh, A., “Similar Thrust Performance in Diverging-Magnetic-Field Electrostatic Thruster with Monoatomic Propellants,” *Journal of Propulsion and Power*, Vol. 35, No. 1, 2019, pp. 236-238.

[15]Ichihara, D., Uno, T., Kataoka, H., Jeong, J., Iwakawa, A., and Sasoh, A., “Ten-Ampere-Level, Applied-Field-Dominant Operation in Magnetoplasmadynamic Thrusters,” *Journal of Propulsion and Power*, Vol. 33, No. 2, 2017, pp. 360-369.

[16]Shabshelowitz, A., Gallimore, A. D., and Peterson, P. Y., “Performance of a Helicon Hall Thruster Operating with Xenon, Argon, and Nitrogen,” *Journal of Propulsion and Power*, Vol. 30, No. 3, 2014, pp. 664-671.

[17]Fujita, D., Kawashima, R., Ito, Y., Akagi, S., Suzuki, J., Schönherr, T., Koizumi, H., and Komurasaki, K., “Operating Parameters and Oscillation Characteristics of an Anode-Layer Hall Thruster with Argon Propellant,” *Vacuuum*, Vol. 110, 2014, pp. 159-164.